Research Article

Pham Van Dong, Nguyen Huu Phan*, Nguyen Van Thien, Nguyen Huy Kien, Tran Quoc Hung, Nguyen Mai Anh, Hoang Xuan Thinh, and Hoang Van Nam

Enhancing the machinability of SKD61 die steel in power-mixed EDM process with TGRA-based multi criteria decision making

https://doi.org/10.1515/jmbm-2022-0039
received April 06, 2022; accepted May 21, 2022

Abstract: In the current context, an attempt is being made to improve the electrical discharge machining (EDM) process by using powder particles in a suitable combination. To improve the quality of such procedures, the process parameters should be optimized. The present study proposes to utilize Taguchi–Grey relational analysis to discover the optimal combination of process parameters for SKD61 die steel specimens using titanium powder-mixed EDM (PMEDM). Among the machining parameters chosen, the optimal combination of current (3 A), pulse on-time (37 μs), pulse off-time (37 μs), and powder concentration (4 g/L) was determined experimentally. Due to its relevance in spark energy production, peak current is a more significant factor in PMEDM processes. A superior surface topography was obtained with increased microhardness and fewer microfractures over machined specimens with optimal process parameter in PMEDM. The titanium particles can effectively enhance the surface performance measures during PMEDM-based machining owing to tiny craters and pores with better lubrication.

Keywords: SKD61, die steel, PMEDM, TGRA

1 Introduction

Electrical discharge machining (EDM) utilizes the thermal energy generated by electrical discharge sparks to attack the machined surface continuously and repeatedly. During the machining operation, the materials in the workpiece and electrode are melted and evaporated [1]. Allowing the deionization of the pressurized dielectric medium ejects the resolidified particles from the machining zone [2]. Additionally, it may influence the thermal and electrical conductivity of the plasma generated in the machining zone. The dielectric medium's characteristics can affect both the formation of craters and microcracks and the thickness of the white layer [3]. To establish the surface layer's quality, the roughness (R_a), hardness (HV), average white layer thickness (WLT), and heat-impacted zone were measured (HIZ). As a result, the cost of machining has grown dramatically, as has tool material wear [4]. As a result, optimizing the surface layer quality throughout the EDM process continues to be a difficulty. Numerous variables, such as electrical settings, electrode materials, and dielectric fluid, can affect the EDM process's surface quality. Numerous parameters, such as current (I), pulse-on time (T_{on}), and pulse-off time (T_{off}), all influence the surface quality during the EDM process. Additionally, these variables can impact the recast layer's depth [5]. The EDM procedure of removing the WLT layer from the machining surface is time consuming. Reduce the depth of the WLT to increase the surface quality. Electrical resistivity and thermal conductivity of the insulating medium might potentially affect surface performance evaluations during the EDM process [6]. Additionally, the machined workpiece's surface quality is determined by the tool wear rate (TWR), which is greatly influenced by the specific gravity, tensile strength, electrical conductivity, and melting temperature of the electrode materials. In EDM operations with low surface quality, water-diluted dielectric fluid is more productive than oil-diluted dielectric fluid [7]. The diameter of the crater is mostly determined by the nature of the dielectric medium. Microcracks vary in length and distribution depending on the heat conductivity of the workpiece [8]. However, fabricating electrodes with complicated shapes with these materials

* **Corresponding author: Nguyen Huu Phan,** Hanoi University of Industry, No. 298, Cau Dien Street, Bac Tu Liem District, Hanoi, Vietnam, e-mail: phanktcn@gmail.com
Pham Van Dong, Nguyen Van Thien, Nguyen Huy Kien, Tran Quoc Hung, Nguyen Mai Anh, Hoang Xuan Thinh, Hoang Van Nam: Hanoi University of Industry, No. 298, Cau Dien Street, Bac Tu Liem District, Hanoi, Vietnam

is extremely difficult. Powder-mixed EDM (PMEDM) can be used to eliminate microfractures and voids in the WLT [9]. The electrode material and composition of the powder used with the dielectric fluid during the PMEDM process may affect the machined surface's WLT [10]. During the EDM process, a stronger tool electrode can provide a smoother surface with a higher surface hardness. Additionally, the particle size of the powder material may affect the depth of the WLT, which in turn affects the high voltage of the machined surface during the EDM process [11]. Powder particle size has a significant effect on the capabilities of machined specimens to withstand high voltage [12]. In comparison to standard EDM, PMEDM considerably lowers particle adherence and small fractures [13]. It was revealed that the particle size of the powders mixed with the dielectric medium has an effect on the PMEDM process's efficacy [14]. The powder-mixed dielectric medium can be used as an insulating medium. It can increase the efficiency and surface quality of machined specimen as compared with the conventional EDM process [15]. The addition of conductive powders can reduce the resistance of dielectric fracture to reduce the machining time with better surface quality in the PMEDM process [16]. This has created considerable research directions to improve the machinability of titanium alloy in the PMEDM process. Silver nano powder-mixed dielectric solution has resulted in better measures of EDM process while machining titanium specimens [17]. It could provide higher machining operating cost in such process. The lower WLT was observed in the PMEDM process. Many factors such as powder types, concentration, and size were contributed to assess performance measures in the PMEDM process [18]. It was also observed that the chromium nano-sized particles have efficiently contributed than micron-sized chromium particles in the PMEDM process. Nevertheless, the chromium nano powders used in PMEDM resulted in four times higher production costs as that of micro chromium powders. The quality indicators in PMEDM using Al_2O_3 powder mixed with different dielectric fluids were analyzed and evaluated [19]. The higher material removal rate (MRR) was observed with transformer oil as dielectric medium than distilled water in the PMEDM process. The lower electrode-wear-rate (EWR), surface-roughness (R_a), and radial-overcut (ROC) were observed with kerosene dielectric medium. The MRR, R_a, and WLT have been significantly improved in PMEDM with B_4C powder while machining titanium (Ti-6Al-4V) alloy [20]. The MRR was significantly improved with lower R_a and WLT using SiC powder on machining titanium (Ti-6Al-4V) alloy [21]. While utilizing chromium particles combined with dielectric medium, the hardness of the layer increased two times during the machining of AISI D2 steel in the PMEDM process. The size of the cracks, craters, and adhesion particles on the machining surface were significantly reduced in the PMEDM process while compared with the EDM process [22]. It was inferred that usage of different particles with the insulating medium could enhance the surface measures of the EDM process [23]. The mechanism of the machining process can be enhanced by including the electrical conductive powders in the dielectric medium owing to the modification of electrical conductivity of plasma column [24]. The particles could be distributed uniformly by incorporating the magnetic stirrer in the process. The addition of B_4C-based ceramic particles in the dielectric medium can efficiently enhance the process mechanism [25]. The utilization of mixing the tungsten carbide particles with dielectric medium can improve the surface performance measures while machining titanium alloy [26]. The size of powder material can also modify the depth of WLT which can change the HV of machined surface in the EDM process. The graphite powder produces larger crater radius owing to the higher thermal energy of each spark over the workpiece [27]. The surface hardness of various mold steels such as D3, H113, and D6 has been significantly improved by PMEDM using Mn, Al, and Al–Mn powders. The size of the powder materials can strongly affect the HV of machined specimens [28]. A composite layer has been created over the machined surface due to the penetration of a significant amount of powder materials and thus contributed to significantly improve its mechanical properties [29]. A layer of nitrite was found over the machined AISI 4140 steel surface with Cu and Graphite electrode, under the mixture of urea and deionized water [30]. The effectiveness of powders such as Al, SiC, and Al_2O_3 mixed dielectric fluid could modify the various quality measures of MRR, TWR, and over cut in an efficient manner [31]. It was found that the size of the powders mixed with dielectric medium can further alter the effectiveness of the PMEDM process [33].

The surface should be as high quality as possible in terms of structure. This can be performed by implementing multi-response optimization techniques, sometimes known as multi-criteria decision-making (MCDM) approaches. It is necessary to develop MCDM in order to determine the ideal parameter combination for the PMEDM procedure [32]. Numerous strategies exist for converting several response characteristics into a single performance measure in any process [33]. Weight assignment, genetic algorithms (GA), the Taguchi data envelopment analysis ranking approach, and Taguchi–Grey relation analysis (TGRA) are among these techniques. The response

surface methodology has been used to optimize parameters in virtually any industrial process in order to quantify their effect. Regardless of the method, a MCDM strategy based on the Technique of Order Preference Similarity to the Ideal Answer may provide a more technical solution than prior technologies. Multi-objective optimization method by ratio analysis is a strategy based on ratio analysis for optimizing multiple objectives [34]. It was created to address multi-objective challenges in any process by utilizing the principal component analysis technique. GA, ant colony optimization, and the Preferential Selection Index are key [35]. TGRA has the potential to significantly improve the mechanism of action of the procedure. However, the computation's precision can be adjusted by adjusting the gray-scale coefficient. TGRA is often used due to its enhanced efficacy and versatility. The TGRA technique has been shown to be effective for determining the optimal mix of components for any manufacturing process [36]. The TGRA technique can be used to determine the ideal process parameters, whose significance dictates how machining processes respond. Only MCDM can create superior process factors in machining processes, according to the entire survey.

After conducting a review of the literature, it was revealed that just a few research attempts had been made to incorporate MCDM into the PMEDM process. It was discovered that little effort has been made to optimize the process parameters for PMEDM machining of SKD61 die steel. The current study was initiated as a result of this discovery. The current study used a TGRA-based MCDM technique to machine SKD61 die steel in the PMEDM process. Additionally, the PMEDM technique was used to investigate the impacts of powder particles on the machined surface quality metrics topography, microcracks, WLT, R_a, and HV.

2 Experimental methodologies

2.1 Choice of workpiece and process factors

Due to its importance in the creation of complex-form hot stamping dies for manufacturing applications, the present study selected SKD61 die steel specimens with a sample size of 45 mm × 27 mm × 10 mm as the workpiece specimens. The machining trials were performed using an AG40L electrical discharge machine (Sodick, USA) equipped with a powder mixing stirrer configuration similar to that shown in Figure 1. EDM drilling was used to make blind holes 50 mm in diameter above the specimens. Titanium powder particles were deemed powder particles in this experiment because of their electrical and thermal conductivity. Titanium powder was selected due to its excellent conductivity, low specific gravity, and nonmagnetic characteristics. The particles had an average diameter of 45 µm and were mixed with HD-11 oil dielectric fluid at a flushing pressure of 10 L/min and with the tool electrode polarized positively. We used a copper (Cu) tool electrode with a 22 mm diameter. Experiments were conducted using the process parameter combinations shown in Table 1.

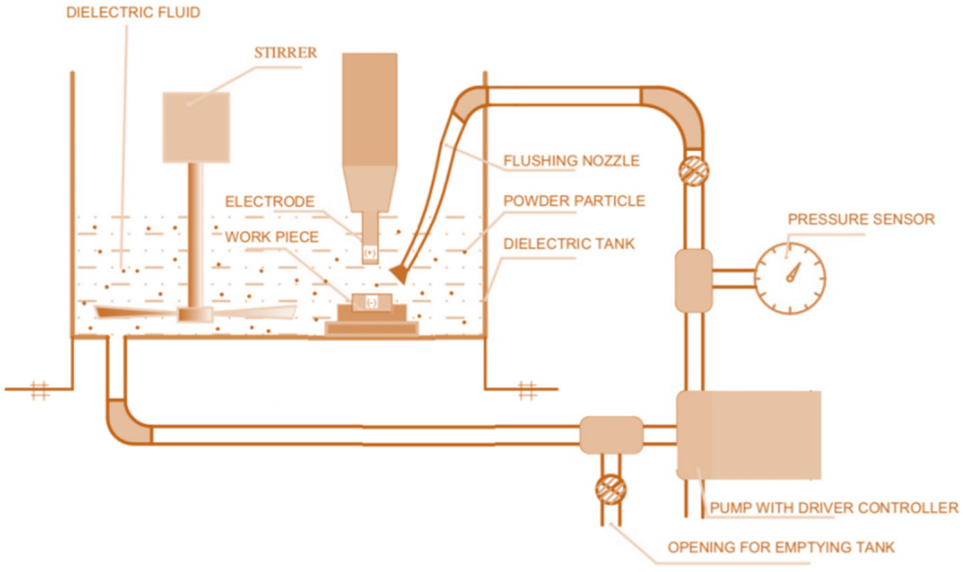

Figure 1: Experimental scheme used in the present study.

Table 1: Selection of process parameters

Process parameters	Symbol	Unit	Variables
Peak-current	I	A	1, 2, 3
Pulse on-time	T_{on}	μs	18, 25, 37
Pulse off-time	T_{off}	μs	18, 25, 37
Powder concentration	C	g/l	3, 4, 5

The process variables were chosen to represent the process parameters at their maximum, medium, and minimum values.

In this investigation, HD-1 dielectric fluid was employed, since it has frequently been utilized in Vietnam for current pulse processing. Two stirring vanes were turned in opposite directions at a speed of 200 rev/min to ensure that the titanium powders were distributed uniformly throughout the dielectric. A solvent pump was employed to maintain a constant flow rate of 24 L/min into the processing chamber. The magnets were employed to attract debris formed during the machining process and preventing it from combining with the titanium powder. The entry of such particles entering the machining zone would have harmed the electrical discharge process. The dielectric fluid performs a variety of purposes, including preventing discharges, cooling the operation, and expelling undesirable material from the cutting zone. The dielectric fluid used is determined by the application and the cost of production.

2.2 Measurement of quality measures

The MRR, the TWR, the surface roughness (R_a), the microhardness (HV), and the WLT were all used as quality indicators in this experiment. The weights of the workpiece and electrode were determined precisely using a digital weighing scale with an accuracy of 0.001 g and a standard deviation of 10 mg (Model: Vibra AJ-203 SHINKO, Japan). The surface roughness (R_a) was evaluated using a 0.8 mm cutoff length contact probe profilometer (SJ-210) (MITUTOYO, JAPAN). Three measurements were obtained for each test sample, and the average of the three values was utilized. The surface morphology was determined using a JEOL-6490 scanning electron microscope and a Carl Zeiss Axiovert 40MAT optical microscopy. The hardness (HV) was evaluated using a 0.5 kg applied stress on an Indenta Met 1106 microhardness tester (Buehler, USA). According to Muthuramalingam's idea [37], the average thickness of the white layer has been estimated.

3 Results and discussion

In this investigation, SKD61 die steel specimens were machined using the PMEDM method according to the experimental design described in the preceding section, and the findings are summarized in Table 2. Three measurements were obtained for each test sample, and the average of the three values was utilized.

3.1 Effect of I on performance measures

Figure 2 shows the influence of I on the quality parameters in PMEDM using titanium powder. The change of I led to the quality parameters being changed quite strongly, and the increase of I led to the value of the quality indicators being increased accordingly. This may be due to an increase in I leading to an increase in spark

Table 2: Quality measures matrix in PMEDM process

Exp. No	I (A)	T_{on} (μs)	T_{off} (μs)	C (g/l)	MRR (mm^3/min)	TWR (mm^3/min)	R_a (μm)	HV (HV)	WLT (μm)
1	1	18	18	3	12.623	0.519	0.605	911.9	12.72
2	1	25	25	4	13.54	0.506	0.488	978.8	15.7
3	1	37	37	5	17.195	0.451	0.368	918.9	15.766
4	2	18	25	5	18.077	0.753	0.816	1090.6	18
5	2	25	37	3	16.542	0.641	1.04	900.1	19.6
6	2	37	18	4	17.871	0.842	0.943	1047.6	18.8
7	3	18	37	4	20.366	1.029	1.136	1380.8	19.06
8	3	25	18	5	20.435	1.164	0.983	1090.0	21
9	3	37	25	3	19.194	1.626	1.28	980.5	19.72
Mean					17.3159	0.8368	0.8510	1033.24	17.8184
Standard deviation					2.7464	0.3827	0.3069	149.49	2.6016
Standard error					0.9155	0.1276	0.1023	49.83	0.8672

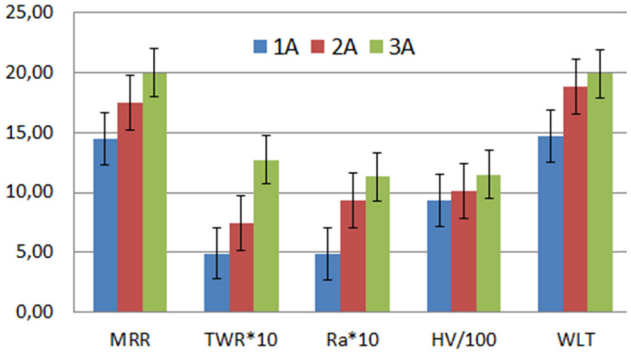

Figure 2: Effect of I on performance measures.

discharge energy. It leads to the thermal energy of the spark impacting the machined surface of the workpiece and the electrode to be greatly increased. Hence, the amount of material of the electrode and the workpiece to be melted and evaporated was also increased. The cause of the increase in WLT could be because the amount of workpiece-powder-electrode adhered to the surface of the workpiece also increased with the increase of I. R_a of the machined surface was also increased by I due to the increase of the size of the craters on the surface of the workpiece. The increase in HV can be attributed to the increased penetration of Titanium powders and Carbon into the machined surface. MRR, TWR, R_a, and WLT were significantly altered with an increase of I, and HV was slightly altered.

3.2 Effect of T_{on} on performance measures

The influence of T_{on} on MRR, TWR, R_a, HV, and WLT in PMEDM using titanium powder is shown in Figure 3. The increase in T_{on} led to an increase of MRR, TWR, and WLT. But the increase of these quality indicators was not significant. This was due to an increase in the energy of the sparks in the PMEDM under T_{on} = 18–37 µs. However, the increase in spark energy was not significant. R_a was changed very little by T_{on} change. The hardness of the machined surface (HV) after PMEDM was reduced by the increase of T_{on} has resulted in a decrease in the amount of titanium powder entering the machined surface. The increase of WLT in PMEDM could be due to the increased adhesion of electrode material, workpiece, and powder material to the machined surface. In general, the change of T_{on} led to the quality indicators in PMEDM being slightly affected.

3.3 Effect of T_{off} on performance measures

The T_{off} in PMEDM affects the process of chips, powders, and dielectric fluid being ejected from the gap at discharge, after they are impacted by sparks. It also affects the recovery of the dielectric fluid and the deposition of powder into the machined surface. Figure 4 shows that the change of quality parameters (MRR, TWR, R_a, HV, and WLT) was not significant with the increase under T_{off} = 18–37 µs. MRR, TWR, and R_a were slightly increased, and MRR increased by 6.8%. The reason may be that the increased T_{off} led to a more stable machining process. Therefore, the useful energy in machining was increased. The HV of the surface layer was increased, it may be because the increase of T_{off} has led to easier process of titanium powder material entering the machined surface. This was also the cause of the increase in WLT.

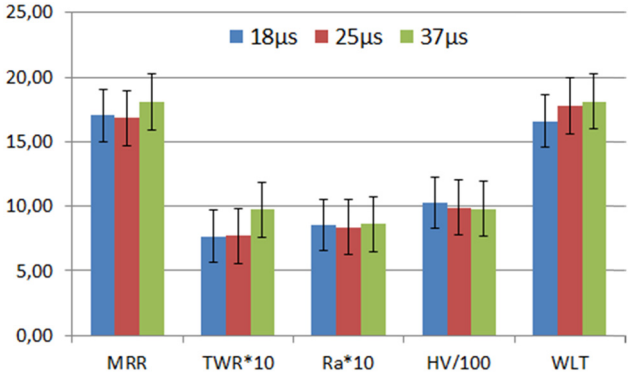

Figure 3: Effect of T_{on} on performance measures.

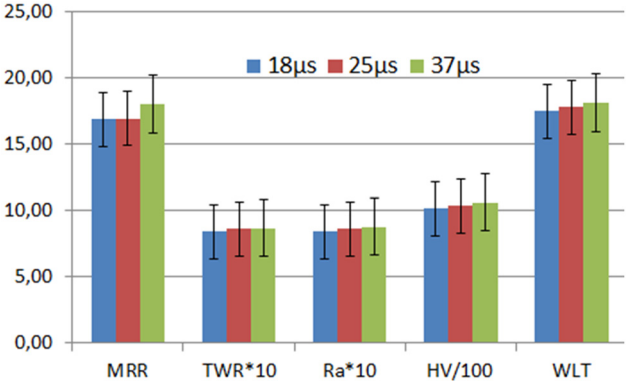

Figure 4: Effect of pulse off time on performance measures.

3.4 Effect of titanium powder concentration (*C*) on performance measures

The addition of powder to the dielectric fluid increased the number of sparks and decreased the energy required to break down the dielectric fluid, hence increasing useable energy. Additionally, the presence of powder particles in the discharge gap results in an increase in the size of the discharge gap. Additionally, it is simpler to remove the chip and dielectric solution from the discharge gap. It may result in more stable machining. Figure 5 illustrates the influence of titanium powder mixed with dielectric fluid on the EDM processing of SKD61. Increases in C = 3–5 g/L resulted in a 15.2% rise in MRR. TWR and R_a were decreased by 15.0 and 25.91%, respectively. The reason for this could be that the number of sparks increases, resulting in a drop in the energy of each spark. The rise in powder concentration resulted in an increase in powder accessing the workpiece surface layer following PMEDM, and WLT increased marginally (5.23%) at C = 5 g/L. The hardness of the surface layer changed insignificantly (≈10.73%), and the HV was maximum at C = 4 g/L. However, the value of powder concentration is too high, it will lead to more occurrence of short-circuit phenomenon. Hence, the machining process is not stable. It can negatively affect the improvement of quality indicators in PMEDM.

3.5 Multi-response optimization of process parameters by TGRA

In the present study, TGRA-based MCDM technique was applied to machine SKD61 die steel in the PMEDM process. Figure 6 illustrates rules involved in TGRA methodology.

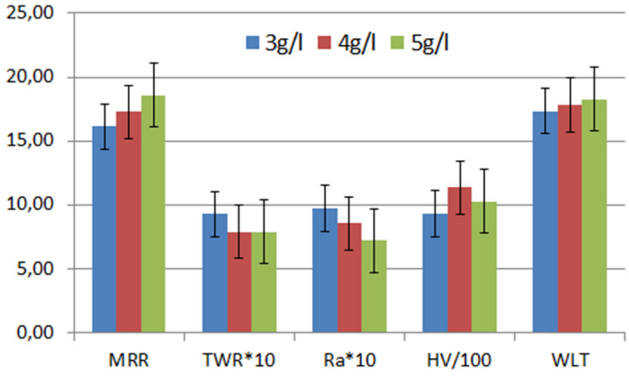

Figure 5: Effect of titanium powder concentration on performance measures.

The signal to noise (S/N) ratios and their normalized values (N-S/N) for the specified quality measurements in the PMEDM process are shown in Table 3. MRR and HV should be increased, while TWR, R_a, and WLT should be decreased, in order to achieve higher performance metrics in the PMEDM process. Given that the current inquiry required both features, 0.5 was chosen. The G_n value for each trial is listed in Table 4. This higher G_n value suggests a more efficient MCDM in the PMEDM process. The mean G_n values for all input factor levels are shown in Table 5. As a result, the more advantageous process factors are those with a higher mean G_n value in the process. As a result, the ideal parameters were identified in the study, as indicated in Table 5. The max–min relationship demonstrated that the key determining factor on quality metrics in the PMEDM process was the maximum–minimum relationship. The spark energy used in the PMEDM process has an effect on the amount of material removed from the workpiece and tool electrode. The roughness of the surface is mostly determined by the crater formation, its size, and dispersion. The size of the crater is determined by the peak current. Thermal energy is responsible for the development of the WLT. Peak current may have an effect on the production of spark plasma during the PMEDM process. As a result, the current plays a critical role in assessing the quality metrics used in the PMEDM process. After computing the optimal factor combination, a confirmation test was run to determine its confidence. It was noted that the G_n grade value improved by 3.4% when compared to the Ge.

Confirmation Experiments: Confirmation experiments were carried out using the optimal process parameters such as the material workpiece (SKD61), material electrode (Cu), reverse polarity, pulse-on time (37 µs), current (3 A), pulse-off time (37 µs), and concentration (4 g/L). The results of the experiment are shown in Table 6. The coefficient of gray levels obtained from the experimental results at optimal process parameters was the largest. Compared with the results of the best experiment (7st), the optimal efficiency is improved by 10.81%. This showed that the processing efficiency improved significantly.

3.6 Surface morphology of the machined specimens under optimal factor setting

The observation of the analytical image of the compound organization on the machined surface layer showed that the carbide of titanium – carbon and alloy of

Calculation of S/N ratio:

- Smaller-the-better characteristics

$$\frac{S}{N}\ ratio = -10\log\frac{1}{m}\sum Y_{ab}^2$$

- Larger-the-better characteristics

$$\frac{S}{N}\ ratio = -10\log\frac{1}{m}\sum 1/Y_{ab}^2$$

m - Number of experimental replication
Y_{ab} - Response of ath trial of bth dependent level.

Calculation of normalized *S/N* ratio:

- Smaller the better characteristics

$$Z_{ab} = \frac{\max(Y_{ab}) - Y_{ab}}{\max(Y_{ab}) - \min(Y_{ab})}$$

- Larger the better characteristics

$$Z_{ab} = \frac{Y_{ab} - \min(Y_{ab})}{\max(Y_{ab}) - \min(Y_{ab})}$$

Z_{ab} - Normalized of a^{th} trial of b^{th} dependent level.

Computation of grey co-efficient (*GC*):

$$GC_{ab} = \frac{(\Psi_{min} + \delta\Psi_{max})}{(\Psi_{ab} + \delta\Psi_{max})}$$

Ψ_{ni} - Grey co-efficient for a^{th} trial of b^{th} dependent response; $\Psi = 1 - Normalized\ S/N$

δ - Distinctive co-efficient's value is from 0 to 1

[In the present study, δ is considered as 0.5 due to LTB and STB characteristics of quality measures]

Computation of grey relation grade (G_n):

$$G_n = \frac{1}{M}\sum GC_{ab}$$

M - Number of the performance measures

Confirmation experiment:

$$G_e = G_f - \sum(G_h - G_f)$$

G_e – Predicted GR grade
G_f–Total averageGR grade
G_n–Optimal average GR grade

Figure 6: TGRA-based methodology in PMEDM process.

Table 3: Normalized ratio of the present study

Trial	S/N ratio					N-S/N ratio				
No	MRR	TWR	R_a	HV	WLT	MRR	TWR	R_a	HV	WLT
1.	22.0233	5.6967	4.3649	59.1990	−22.0897	0	0.1095	0.3988	0	0
2.	22.6324	5.9170	6.2316	59.8139	−23.918	0.1456	0.08973	0.2264	0.1706	0.4198
3.	24.7080	6.9165	8.6830	59.2654	−23.9544	0.6416	0	0	0.0184	0.4282
4.	25.1425	2.4641	1.7662	60.7533	−25.1055	0.7455	0.3997	0.6388	0.4313	0.6925
5.	24.3718	3.8628	−0.3407	59.0858	−25.8451	0.5613	0.2741	0.8334	−0.0314	0.8624
6.	25.0430	1.4938	0.5098	60.4039	−25.4832	0.7217	0.4868	0.7549	0.3344	0.7793
7.	26.1781	−0.2483	−1.1076	62.8026	−25.6025	0.9930	0.6432	0.9043	1	0.8067
8.	26.2075	−1.319	0.1489	60.7485	−26.4444	1	0.7394	0.7882	0.4300	1
9.	25.6633	−4.2224	−2.1442	59.8290	−25.8981	0.8699	1	1	0.1748	0.8746

Table 4: Gray relational grade of the present study

Trial No	GC grade					Gray relational grade
	MRR	TWR	R_a	HV	WLT	
1.	0.3333	0.3596	0.4541	0.3333	0.3333	0.3627
2.	0.3692	0.3545	0.3926	0.3761	0.4629	0.3911
3.	0.5825	0.3333	0.3333	0.3375	0.4665	0.4106
4.	0.6627	0.4544	0.5806	0.4679	0.6192	0.5570
5.	0.5326	0.4079	0.7501	0.3265	0.7842	0.5603
6.	0.6424	0.4935	0.6710	0.4290	0.6937	0.5859
7.	0.9861	0.5836	0.8393	1	0.7211	0.8260
8.	1	0.6573	0.7025	0.4673	1	0.7654
9.	0.7936	1	1	0.3773	0.7994	0.7941

Table 5: Computation of optimal process parameters combination

Factors	L1	L2	L3	Optimal parameters	Max–Min
I	0.3881	0.5677	0.7952	3 A	0.4070
T_{on}	0.5819	0.5722	0.5969	37 µs	0.0246
T_{off}	0.5714	0.5807	0.5990	37 µs	0.0276
C	0.5724	0.6010	0.5777	4 g/L	0.0287

Table 6: Results of confirmation experiments

Machining characteristics	Exp. value		
	7st	Optimal parameters	Difference (%)
MRR (mm^3/min)	20.366	21.882	2.53
TWR (mm^3/min)	1.029	0.853	-17.05
SR (µs)	1.136	0.93	-18.13
HV (HV)	1380.8	1213.7	-12.10
WLT (µs)	19.06	19.81	3.93
Gray relational grade	0.8260	0.9153	10.81

Fe – titanium had formed on the white layer (Figure 7). These organizations can improve the workability of the machined surface after PMEDM. With the special properties of titanium, titanium carbides, and Ti-Fe alloys, the mechanical properties of the machined surface can be greatly improved according to the wear resistance, corrosion resistance, and thermal stability. The titanium powder material was melted and evaporated by the electric spark and it has penetrated the surface layer of the workpiece. The analysis results of elemental composition at different positions of the white layer showed that titanium was distributed quite evenly (Figure 8). The composition of the carbon in the white layer is greatly increased, which was produced by the cracking of the oil fluid dielectric. Titanium, carbon, and copper have penetrated deep into the surface layer. However, the analysis results show that Cu, Ti, and C only appear on the white layer. The topography of the machined surface changed with the change of powder concentration as shown in Figure 9. The number of craters increased with the increase of the powder concentration; however, the size of the craters decreased. The bottoms and mouths of the craters are formed in the form of curved arcs (Figure 10). The cause may be due to the immediate impact of the dielectric fluid on the liquid metal region; it is generated by the spark that hits the surface of the workpiece. The shape of the craters will contribute to improved fatigue resistance of the surface layer compared to other traditional machining methods. Many pores also appear on the surface machined by PMEDM (Figure 11). The size of the craters and pores is small. Those effects can have a beneficial effect on the working condition of the die surface. These craters and pores facilitate the storage of lubricants such as dielectric fluid and lubricating powder during the working life of the product. In addition, microcracks in the machined surface can adversely affect the fatigue resistance of the machined surface layer as shown in Figure 12. On the contrary, it can be highly effective for surfaces subject to sliding friction, because they can create an increase in the adhesion of the lubricant on the machined surface. The number of microcracks increased with the increase of powder concentration, whereas their size decreased. This may be due to the reduction of the spark energy formed in the PMEDM. The analytical characteristics of the white layer have shown that its microscopic hardness cannot be significantly increased. The results showed that the surface layer machined after PMEDM was significantly improved. It is intended to improve the surface quality of mould steel by PMEDM using titanium powder. However, the practical application of this technical solution in practice needs to be based on the working conditions of each type of product.

4 Conclusions

The present work used TGRA-based MCDM optimization to determine the ideal combination of process parameters for machining SKD61 die steel in titanium-based PMEDM. The following conclusions have been drawn from the experiments.

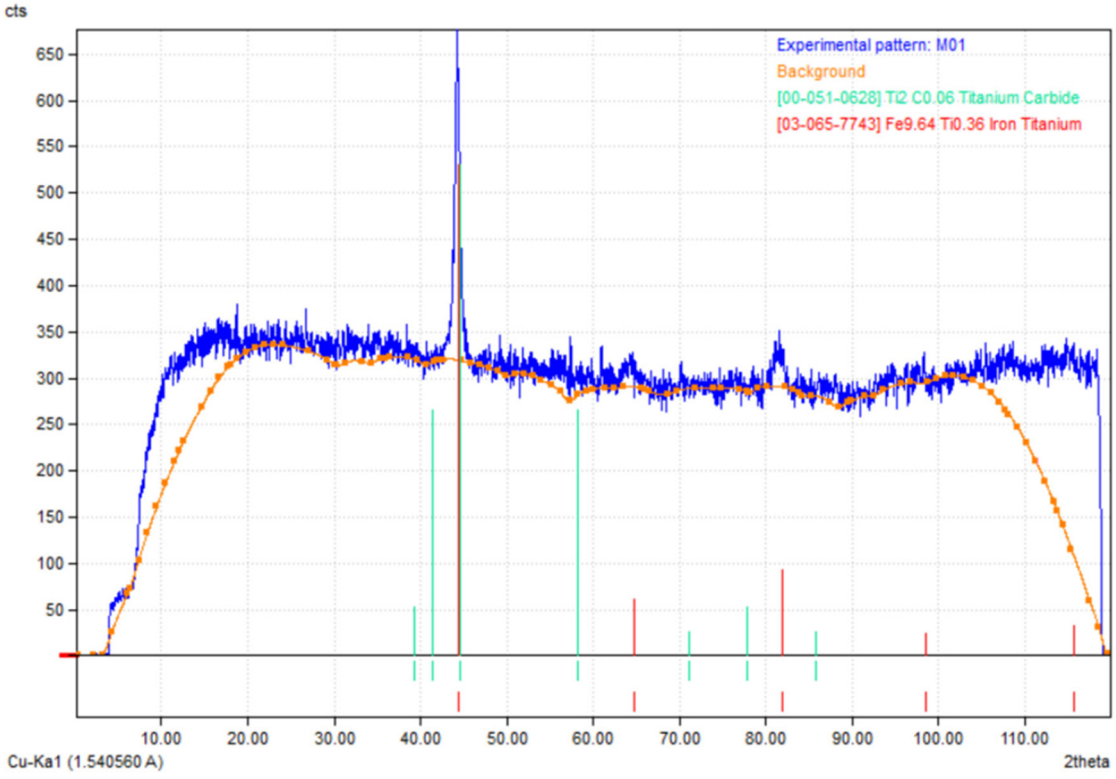

Figure 7: X-ray of white layer.

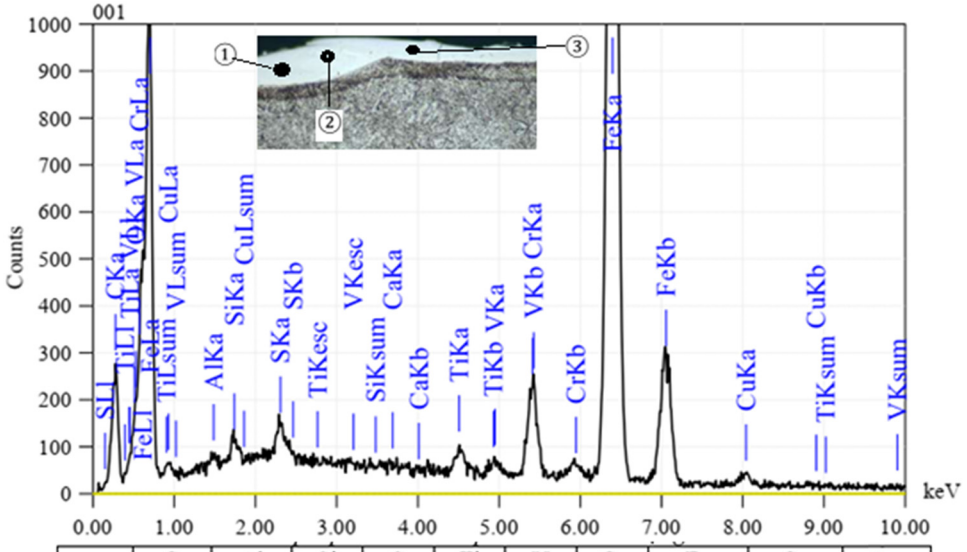

	C	Al	Si	S	Ti	V	Cr	Fe	Cu	Sum
①	12.10	0.22	0.49	0.39	2.41	0.47	4.07	77.60	1.42	100.00
②	11.34	0.08	0.56	0.62	1.85	0.61	3.93	78.85	1.43	100.00
③	10.14	0.14	0.48	0.44	2.09	0.38	4.13	79.83	1.75	100.00

Figure 8: EDAX analysis of machined surface.

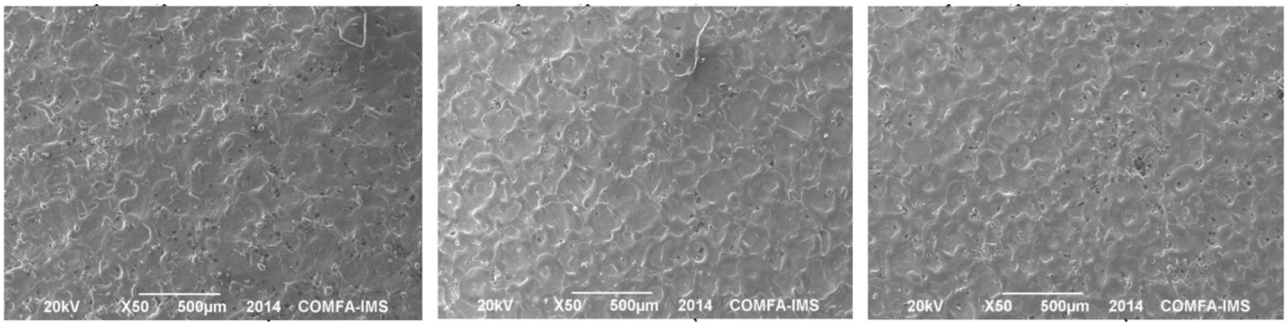

(a) (b) (c)

Figure 9: Topography of machined surface. (a) Topography of machined surface with 3 g/L, (b) topography of machined surface with 4 g/L, and (c) topography of machined surface with 5 g/L.

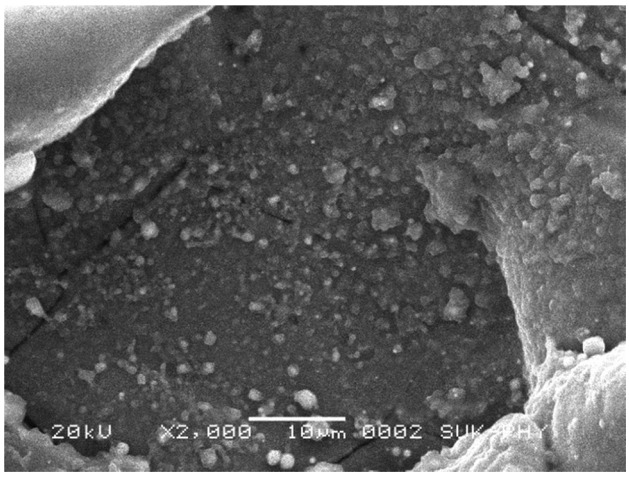

Figure 10: Shape of the craters.

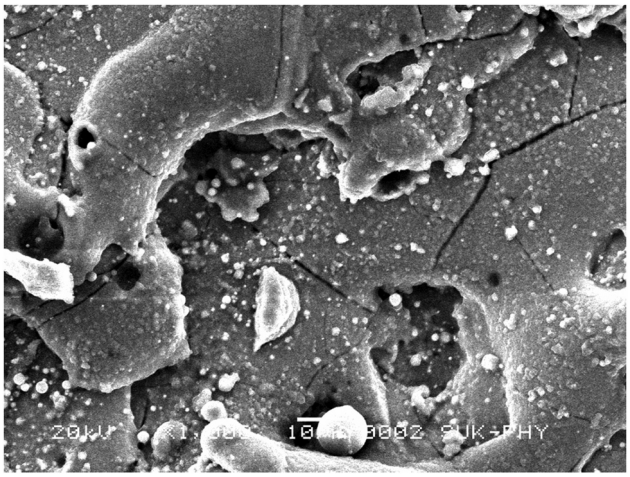

Figure 12: Cracks of machined surface.

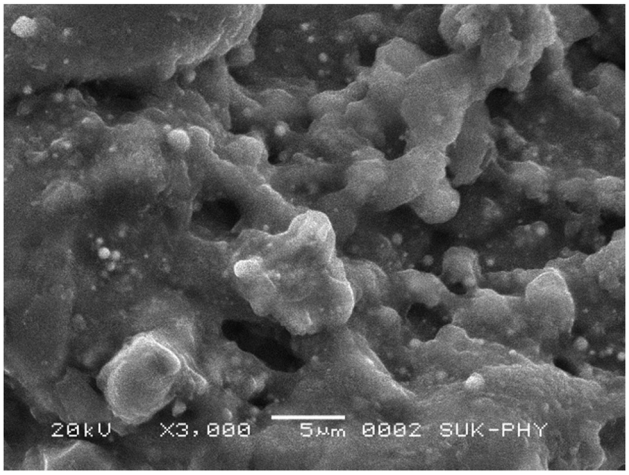

Figure 11: Pores of machined surface.

- The best combination of process parameters in the PMEDM process was determined to be current (3 A), pulse on-time (37 µs), pulse off-time (37 µs), and powder concentration (4 g/L).
- Due to the importance of spark energy in the PMEDM process, the peak current is a more prominent factor.
- Titanium particles can significantly improve surface performance during PMEDM-based machining due to their small craters and pores that provide improved lubrication.
- Under ideal process parameter combinations, a higher HV with fewer microcracks can be achieved over machined specimens.

Funding information: This research was funded by the Ministry of Industry and Trade of The Socialist Republic of Viet Nam.

Author contributions: All authors have accepted responsibility for the entire content of this manuscript and approved its submission.

Conflict of interest: There is no competing interests to be mentioned in the present study.

Data availability statement: There is no need to mention the availability of data and materials in the present study.

Ethical approval: There is no ethical approval needed in the present study.

Consent to participate: There is no consent to participate needed in the present study.

Consent to publish: There is no consent to publish needed in the present study.

References

[1] Muthuramalingam T, Mohan B, Rajadurai A, Prakash MDAA. Experimental investigation of iso energy pulse generator on performance measures in EDM. Mater Manuf Process. 2013;28(10):137–1142.

[2] Muthuramalingam T, Ramamurthy A, Sridharan K, Ashwin S. Analysis of surface performance measures on WEDM processed titanium alloy with coated electrodes. Mater Res Express. 2018;5(12):126503.

[3] Phan NH, Muthuramalingam T, Ngo NV, Nguyen QT. Influence of micro size titanium powders mixed dielectric medium on surface quality measures in EDM process. Int J Adv Manuf Technol. 2020;109(3-4):797–807.

[4] Prihandana GS, Mahardika M, Sriani T. Review micromachining in powder-mixed micro electrical discharge machining. Appl Sci. 2020;10:379.

[5] Yu YT, Hsieh SF, Lin MH, Huang JW, Ou SF. Effects of gas-assisted perforated electrode with rotation on the machining efficiency of PMEDM of titanium. Int J Adv Manuf Technol. 2020;107:1377–86.

[6] Qudeiri JEA, Saleh A, Ziout A, Mourad AHI, Abidi MH, Elkaseer A. Advanced electric discharge machining of stainless steels: assessment of the state of the art, gaps and future prospect. Materials. 2019;12:907.

[7] Vijaykumar SJ, Bagane S. Thermo-electric modelling, simulation and experimental validation of powder mixed electric discharge machining (PMEDM) of BeCu alloys. Alex Eng J. 2018;57:643–53.

[8] Bui VD, Mwangi JW, Meinshausen AK, Mueller AJ, Bertrand J, Schubert A. Antibacterial coating of Ti-6Al-4V surfaces using silver nano-powder mixed electrical discharge machining. Surf Coat Technol. 2020;383:125254.

[9] Hameed AS, Hamdoon FO, Jafar MS. Influence of powder mixed EDM on the surface hardness of die steel. Mater Sci Eng. 2019;518:032030.

[10] Taherkhani A, Ilani MA, Ebrahimi F, Huu PN, Long BT, Van Dong P, et al. Investigation of surface quality in Cost of Goods Manufactured (COGM) method of μ-Al_2O_3 Powder-Mixed-EDM process on machining of Ti-6Al-4V. Int J Adv Manuf Technol 2021. 2021;116:1783–99.

[11] Kumar A, Mandal A, Dixit AR, Das AK, Kumar S, Ranjan R. Comparison in the performance of EDM and NPMEDM using Al_2O_3 nanopowder as an impurity in DI water dielectric. Int J Adv Manuf Technol. 2018;100:1327–39.

[12] Tang L, Ji Y, Ren L, Zhai KG, Huang TQ, Fan QM, et al. Thermo-electrical coupling simulation of powder mixed EDM SiC/Al functionally graded materials. Int J Adv Manuf Technol. 2019;105:2615–28.

[13] Hosni NAJ, Lajis MA. Experimental investigation and economic analysis of surfactant (Span-20) in powder mixed electrical discharge machining (PMEDM) of AISI D2 hardened steel. Mach Sci Technol. 2019;24(3):398–424.

[14] Kumar H. Development of mirror like surface characteristics using nano powder mixed electric discharge machining (NPMEDM). Int J Adv Manuf Technol. 2015;76:105–13.

[15] Mohal S, Kumar H, Kansal SK. Nano-finishing of materials by powder mixed electric discharge machining (PMEDM): A review. Sci Adv Mater. 2015;7:2234–55.

[16] Liu C, Rashid A, Jahan MP, Ma J. Machining of high aspect ratio micro-holes on titanium alloy using silver nano powder mixed micro EDM drilling. ASME Int Mech Eng Congr Expo Proc. 2019. 2A. IMECE2019-10944, V02AT02A011.

[17] Hosni NAJ, Lajis MA. Experimental investigation and economic analysis of surfactant (Span-20) in powder mixed electrical discharge machining (PMEDM) of AISI D2 hardened steel. J Mach Sci Technol. 2020;24:398–424. doi: 10.1080/10910344.2019.1698609.

[18] Lakshmi TS, Choudhury SS, Sundari KG, Surekha B. Investigation on the effect of different dielectric fluids during powder mixed EDM of alloy Steel. Lect Notes Mech Eng. 2020;1067–75. doi: 10.1007/978-981-15-2696-1_103.

[19] Li L, Zhao L, Li ZY, Feng L, Bai X. Surface characteristics of Ti-6Al-4V by SiC abrasive-mixed EDM with magnetic stirring. Mater Manuf Process. 2017;32:83–6.

[20] Hosni NAJ, Lajis MA. The influence of Span-20 surfactant and micro-/nano-Chromium (Cr) Powder Mixed Electrical Discharge Machining (PMEDM) on the surface characteristics of AISI D2 hardened steel. IOP Conf Ser Mater Sci Eng. 2018;342:012095.

[21] Talla G, Gangopadhayay S, Biswas CK. State of the art in powder mixed electric discharge machining: a review. Proc Inst Mech Eng B J Eng Manuf. 2016;231:2511–26.

[22] Joshi AY, Joshi AY. A systematic review on powder mixed electrical discharge machining. Heliyon. 2019;5:e02963. doi: 10.1016/j.heliyon.2019.e02963.

[23] Jeavudeen S, Jailani HS, Murugan M. Powder additives influence on dielectric strength of EDM fluid and material removal. Int J Mach Mach Mater. 2020;22:47–61.

[24] Kolli M, Kumar A. Assessing the Influence of Surfactant and B_4C Powder Mixed in Dielectric Fluid on EDM of Titanium Alloy. Silicon. 2019;11:1731–43.

[25] Kumar S, Batra U. Surface modification of die steel materials by EDM method using tungsten powder-mixed dielectric. J Manuf Process. 2012;14:35–40.

[26] Anirban B, Ajay B, Kulwinder S. FE simulation and experimental validation of powder mixed EDM process for estimating the temperature distribution and volume removed in single crater. Int J Modeling Sci Comput. 2012;3(2):1250006. doi: 10.1142/S1793962312500067.

[27] Azzam SH, Farouk OH, Mohaned SJ. Influence of powder mixed EDM on the surface hardness of die steel. Mater Sci Eng. 2019;518:032030. doi: 10.1088/1757-899X/518/3/032030.

[28] Rogério FS, Ernane RS, Wisley FS, Alberto AR. Influence of the electrode material on the nitriding of medium carbon steel using sink electrical discharge machining. Int J Adv Manuf Technol. 2017;90:2001–7. doi: 10.1007/s00170-016-9531-2.
[29] Ramesh S, Jenarthanan MP, Bhuvanesh KAS. Experimental investigation of powder-mixed electric discharge machining of AISI P20 steel using different powders and tool materials. Multidiscipline Model Mater Struct. 2018;14(3):549–66.
[30] Kumar S, Singh R, Singh TP, Sethi BL. Surface modification by electrical discharge machining: A review. J Mater Process Technol. 2009;209:3675–87.
[31] Sahu DR, Mandal A. Critical analysis of surface integrity parameters and dimensional accuracy in powder-mixed EDM. Mater Manuf Process. 2020;35:430–41.
[32] Jadam T, Sahu SK, Datta S, Masanta M. Powder-mixed electro-discharge machining performance of Inconel 718: effect of concentration of multi-walled carbon nanotube added to the dielectric media. Sådhanå. 2020;45(135):135. doi: 10.1007/s12046-020-01378-2.
[33] Muthuramalingam T, Vasanth S, Vinothkumar P, Geethapriyan T, Rabik MM. Multi criteria decision making of abrasive flow oriented process parameters in abrasive water jet machining using Taguchi-DEAR Methodology. Silicon. 2018;10(5):2015–21.
[34] Sakthivel G, Saravanakumar D, Muthuramalingam T. Application of failure mode and effects analysis in manufacturing industry- an integrated approach with FAHP – FUZZY TOPSIS and FAHP – FUZZY VIKOR. Int J Product Qual Manag. 2018;24(3):398–423.
[35] Teimouri R, Baseri H. Optimization of magnetic field assisted EDM using the continuous ACO algorithm. Appl Soft Comput. 2014;14:381–9.
[36] Muthuramalingam T. Effect of diluted dielectric medium on spark energy in green EDM process using TGRA approach. J Clean Prod. 2019;238:117894.
[37] Muthuramalingam T. Measuring the influence of discharge energy on white layer thickness in electrical discharge machining process. Measurement. 2019;131:694–700.